

124  
**N90-21350**

# TESTS OF THE ROCKWELL Si:As BACK-ILLUMINATED BLOCKED -IMPURITY BAND (BIBIB) DETECTORS

J. Wolf, U. Grözinger, M. Burgdorf, A. Salama<sup>+</sup> and D. Lemke  
Max-Planck-Institut für Astronomie  
Heidelberg, Germany

## Abstract

Two arrays of Rockwell's Si:As back-illuminated blocked-impurity-band detectors have been tested at the Max-Planck-Institut für Astronomie (MPIA) at low background and low temperature for possible use in the astronomical space experiment ISOPHOT<sup>1</sup>. For these measurements a special test equipment was put together. A cryostat was mechanically modified to accommodate the arrays and special peripheral electronics was added to a microprocessor system to drive the cold multiplexer and to acquire the output data. The first device, a 16x50 element array on a fan-out board was used to test individual pixels with a trans-impedance-amplifier at a photon background of  $10^8 \text{ Ph s}^{-1}\text{cm}^{-2}$  and at temperatures of 2.7 to 4.4 K. The noise-equivalent-power NEP is in the range  $5 - 7 \times 10^{-18} \text{ WHz}^{-1/2}$ , the responsivity is  $\geq 100 \text{ AW}^{-1}(f = 10 \text{ Hz})$ . The second device was a 10x50 array including a cold readout electronics of switched FETs (SWIFET). Measurements of this array were done in a background range of  $5 \times 10^5$  to  $5 \times 10^{11} \text{ Ph s}^{-1}\text{cm}^{-2}$  and at operating temperatures between 3.0 and 4.8 K. The NEP ranges from  $< 10^{-18} \text{ WHz}^{-1/2}$  at the lowest background to  $2 \times 10^{-16} \text{ WHz}^{-1/2}$  at the highest flux. On-chip integration times from 1 ms to 4 s were used for these photometric measurements and bias voltages around 4 V proved to be useful. The dark current was measured to be about 64,000 electrons/s and 16,000 electrons/s at 4.2 K and 3.1 K respectively.

## Test Equipment

For testing the detector arrays, special test equipment has been built, consisting of a liquid helium cryostat, an infrared radiation source and a computer system with special peripheral electronics to drive the device and for data acquisition. This test set-up is schematically shown in figure 1.

---

<sup>+</sup> Present address: Astrophysics Division, ESTEC-SA, Noordwijk, The Netherlands

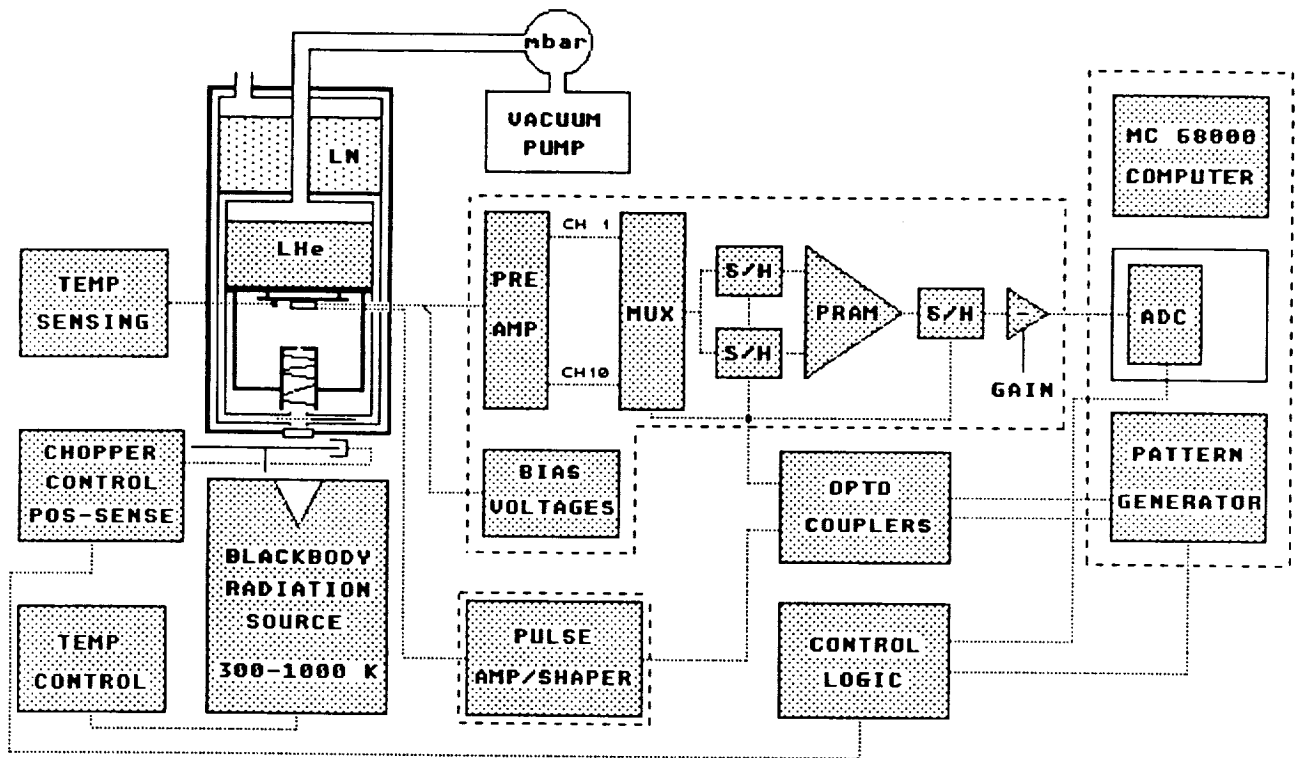


Figure 1 Test Equipment for Detector Arrays

### Cryogenics and Optics

A commercial liquid helium dewar (HD-3, Infrared Laboratories) has been modified as shown in figure 2. An aluminum base plate is bolted to the LHe-tank and carries a pc-board with a 68-pin chip carrier. The test array fits into this chip carrier and is held in place by an aluminum/glass-fibre frame. This frame presses the contacts of the ceramics array substrate against the spring loaded contacts of the carrier. A cold finger of the baseplate penetrates through the pc-board. At its end there is a copper-beryllium spring which provides thermal contact to the ceramics substrate. Additional cooling is provided to the device by the electrical contacts. Copper wires are used from the pc-board to the connectors at the base plate. They are fed through to the bottom of the base plate and are run in milled channels. Thus the wires are in close thermal contact to the helium bath and at the same time light is prevented from leaking into the test housing. The aluminum/glass fibre frame is coupled to the base plate by a strap of braised copper strands. Temperature down to about 2 K can be achieved by pumping on the liquid helium and two carbon resistors are used as temperature sensors at the base plate and the frame.

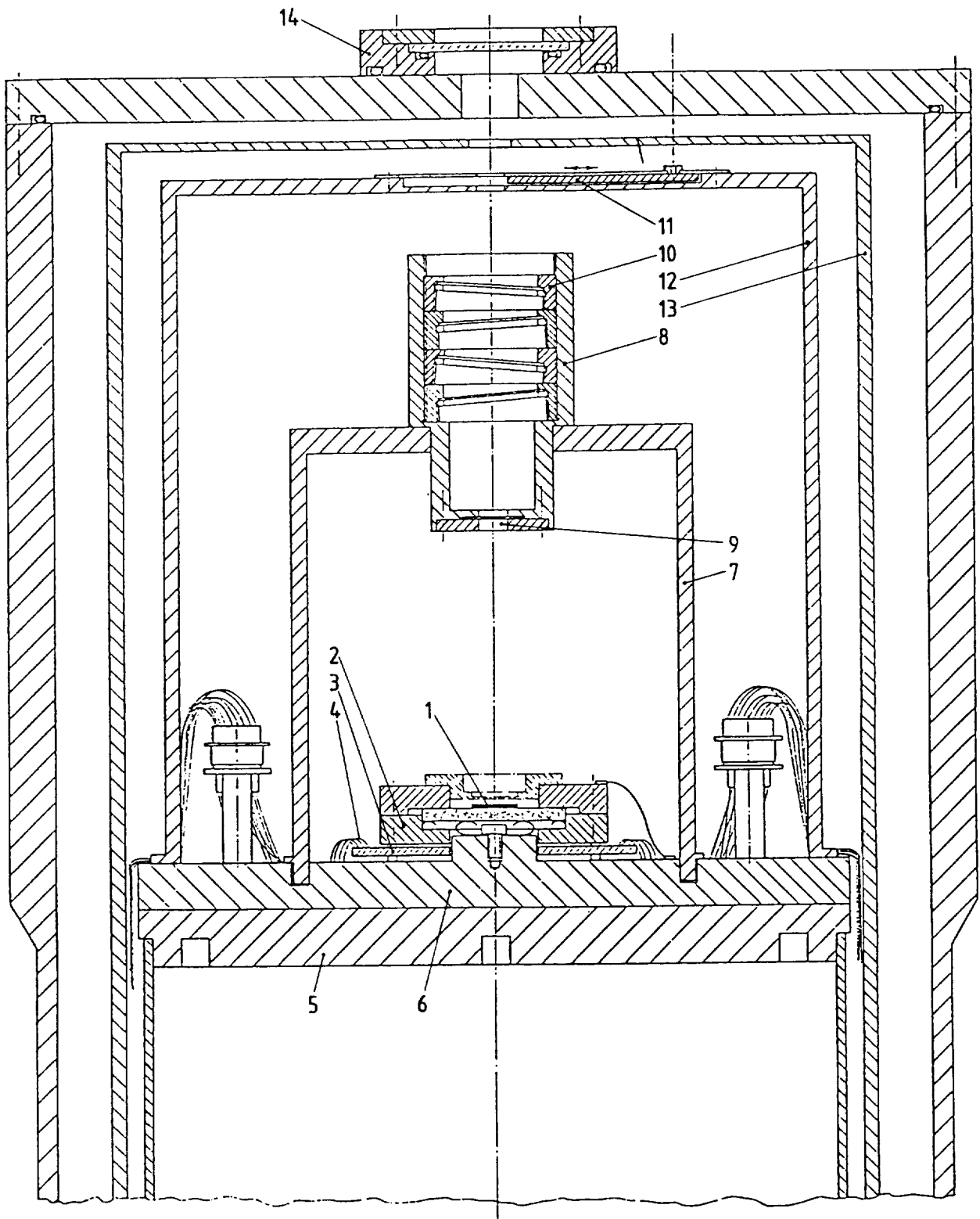


Figure 2      Detector Test Cryostat

A threaded lid covers the base plate light-tight and carries a filter holder. Several spectral and attenuation filters can be mounted into this holder to select the desired infrared flux. The filters are tilt against each other by  $3^\circ$  to avoid multiple reflections between them which could contaminate the beam. A cold aperture of typically 1 mm in diameter in this filter holder defines the field of view of the array.

This test housing is surrounded by a radiation shield at LHe-temperature which contains a shutter to block all light coming into the cryostat. This shutter can be manipulated from outside the dewar with a vacuum feedthrough and is used for dark current measurements or for switching between "0 flux" and radiation entering through the KRS-5 window.

As radiation source a calibrated blackbody with temperature controller is used. Its radiation can be modulated by a rotating chopper wheel at room temperature which can be synchronized to the readout electronics. The fluxes incident on the detectors are calculated using Planck's law and the cold transmission of the filters involved. In chopped operation the signal is the difference of fluxes from the blackbody source and the chopper blade. All numbers of NEP and responsivity given here are calculated at the detector's peak wavelength of 25  $\mu\text{m}$ .

#### Electronics

The 16x50 element array was mounted on a fan-out board and individual pixels could be accessed with a single channel preamplifier. The well known trans-impedance-amplifier, TIA was used with an IRAS module from Infrared Laboratories as an input stage.

The 10x50 element hybrid came with a cryogenic switched FET readout electronics to which the detector array was directly sandwiched. That multiplexer provides one output line for each of the 10 rows. A special electronics system was built to drive the mux and to acquire the output data. For EMC/EMI reasons the system is separated into three parts: a MC 68000 computer system including an analog to digital converter and a pulse generator and two boxes that are directly connected to the electrical plugs of the test dewar. One contains the amplifiers and shaper circuits for the array drive pulses while the sensitive signal processing electronics is located in the second box (see figure 1).

The pattern generator is programmed by the main computer. Once the pulse pattern needed is stored in its RAM, this memory is continuously read out with a selectable speed. No further interaction with the computer is needed. For galvanic separation between analog and digital grounds, the TTL pulses of the pattern generator are fed to the pulse amplifier via opto-couplers. A control logic synchronizes the chopper and triggers the ADC.

The drive pulses needed by the cryogenic multiplexer are generated in the pulse amplifier/shaper box. The upper and lower level of a pulse are defined by two voltage references. An analog switch that is controlled by the pattern generator feeds one of these voltages to an adjustable lowpass filter which is set to provide the desired pulse shapes. A current amplifier is then used as a buffer to provide a low impedance signal to the array (see figure 3). Five such channels are contained in the box.

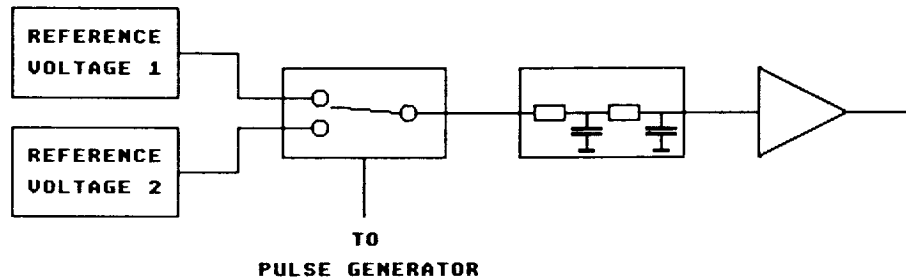


**Figure 3 Pulse Shaper and Amplifier**

The ten output lines of the hybrid are terminated by 10 kΩ resistors and are then fed into a 10-channel preamplifier of gain 16. To apply that gain without saturating the amplifiers, the offset voltage of the signals must first be compensated. This is done by feeding a well filtered DC voltage of a reference source (2.66V) into the inverting input of the operational amplifiers. One of the ten channels is selected by a multiplexer and fed to the inputs of two sample-and-holds which sample the signal and reset levels. The difference of those is then amplified by an instrumentation amplifier where a gain of ten was normally used. This differential signal can be clamped by a third S/H and be additionally amplified by a programmable inverting amplifier which also provides lowpass filtering. It is then fed to the 14-bit analog-to-digital converter of the MC 68000.

Also contained in this "clean" electronics box is the supply for the DC voltages needed by the hybrid. A 10V reference voltage source feeds a set of adjustable voltage dividers. The voltages then go through a buffer amplifier with an active filter and finally to an lowpass RC-filter to ensure stable and very low noise performance.

### TIA Measurements

One pixel of the 16x50 element array was connected to a TIA with feedback resistor of  $R_f = 1.7 \cdot 10^9 \Omega$  (at 4.2K). Some results of these tests are shown in figure 4. Figures 4a and 4b show identical NEP and responsivity taken with different blackbody temperatures.

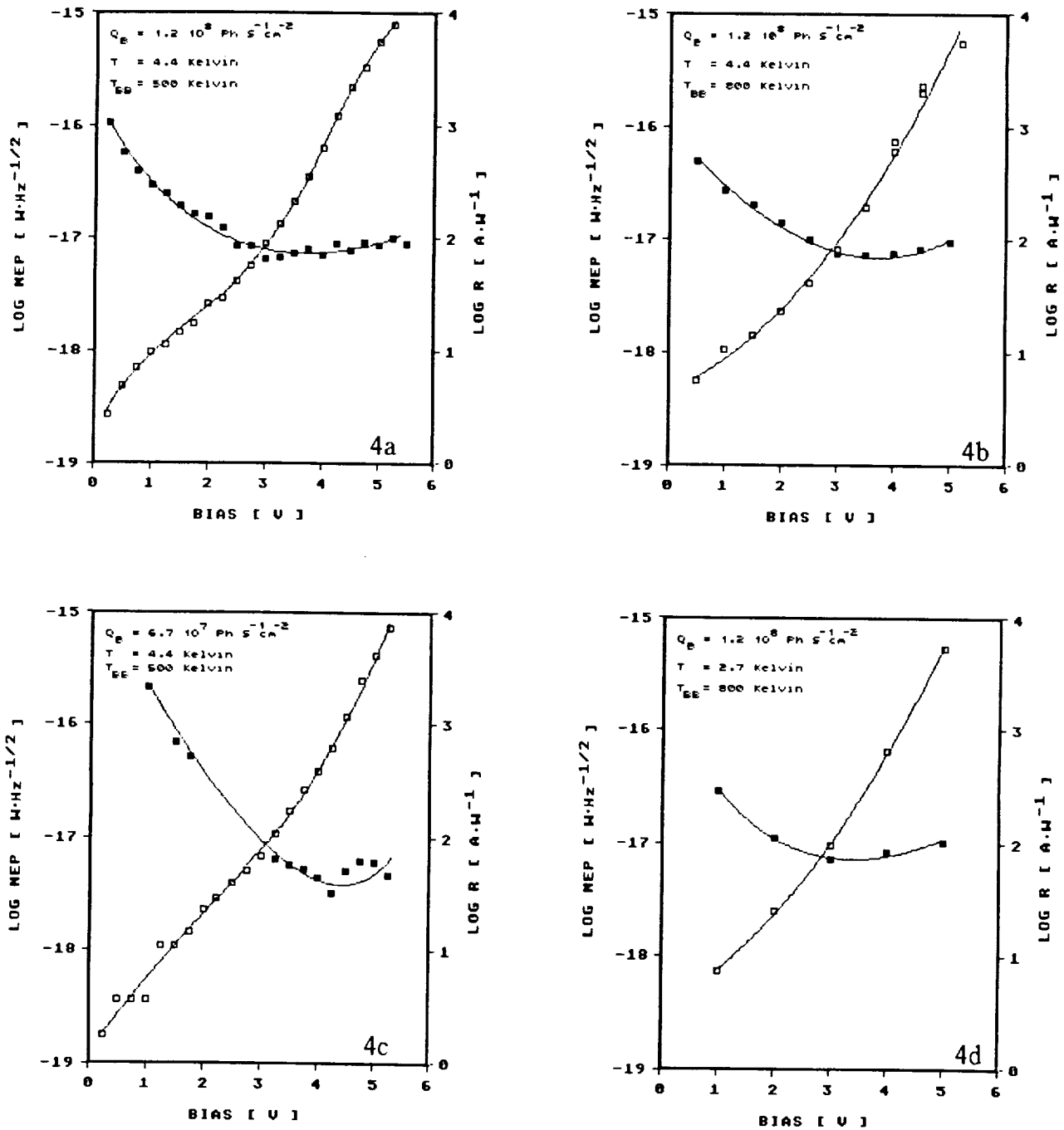


**Figure 4 Testresults of TIA Measurements**

*In the TIA circuit a feedback resistor of  $1.7 \cdot 10^9 \Omega$  which has been calibrated for its non-linearity at temperatures down to 2.7 Kelvin. For the tests in figure 4a,b and d a  $16\mu\text{m}$  cut-on filter was used, for figure 4c a  $13\mu\text{m}$  cut-on was chosen to check the radiometrics. All tests were done with a chopper frequency of 10 Hz.*

This is a first indication that the radiometric calculation and the derived results are reliable. An even better test is the comparison of Figures 4a and 4c. Up to bias voltages of 3.5V the responsivities are identical although completely different cold spectral and attenuation filters were used.

Some deviations between these two responsivity measurements at higher bias voltages could be related to signal drifts. Such drifts were observed after bias switch-on above 3.5V. Their amplitude was within a factor of 2 of the starting point and their time constant at the order of 20 to 30 minutes. As no such effect has been observed in the TIA circuit before, the drift is probably due to the detector.

The NEPs of figure 4a and 4c ratio 7/5 which scales closely with the square root of the background flux ratio, indicating that the NEP is background limited at bias voltages 3 to 4V. Assuming a quantum efficiency of 0.5, the measured responsivity of 100 . . . 200 A·W<sup>-1</sup> (in the bias region of best NEP) gives a photoconductive gain of  $G = 10 \dots 20$ . From this the preamplifier-limited NEP of our TIA is calculated to  $1.9 \cdot 10^{-18} \text{ WHz}^{-1/2}$  which is consistent with our results. Using again  $\eta = 0.5$  background limited NEPs of  $4.3 \cdot 10^{-18} \text{ WHz}^{-1/2}$  for figure 4a and  $3.3 \cdot 10^{-18} \text{ WHz}^{-1/2}$  for figure 4c are found if the photon noise of the background and the signal flux (differential flux blackbody/chopper  $\sim$  photon background) are considered. Our results which are about a factor 1.5 higher indicate an additional noise source in the detector, e.g. gain dispersion. Finally figure 4d indicates that the detector's performance is not changing if it is operated at 2.7 Kelvin.

### Multiplexed Measurements

The test equipment was normally run with the warm multiplexer scanning all ten detector rows, so the data of all 500 elements were taken. By varying background flux, temperature, bias voltage and integration time over a wide range each, huge amounts of data had to be stored. All this data is still available for detailed evaluation, our heavy involvement in the ISOPHOT program however does not allow for that. For this report we have therefore chosen to summarize our results.

Figure 5 shows an example of the NEP and responsivity averaged over the array. At minimum NEP the responsivity is  $\sim 1000 \text{ AW}^{-1}$  if an effective node capacitance of 0.6 pF is assumed<sup>2</sup>. Taking  $\eta = 0.5$  the photoconductive gain is calculated to  $G \sim 100$ . Although this gain is very high, no long time constants are seen. During a 10 minute run after opening the cold shutter at a bias voltage of 3.5V no significant signal drift was observed. Figure 6 gives an overview of the NEP results we got in a wide range of background fluxes.

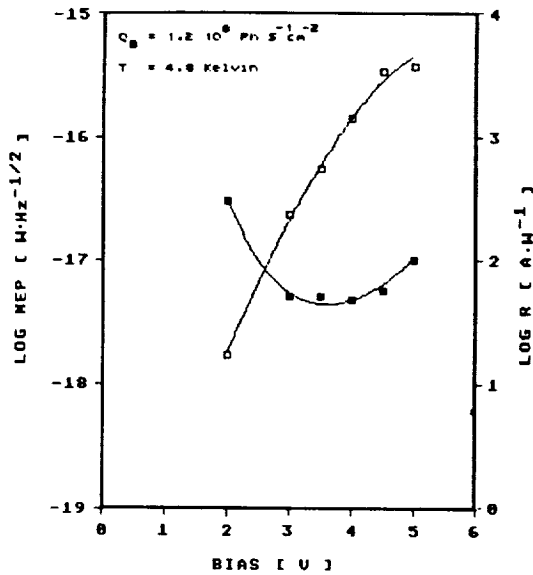


**Figure 5**

**NEP and Responsivity of 10 x 50 Array**

*NEP and responsivity are averaged over all 500 elements. The signal flux is  $1.8 \cdot 10^{-16}$  Watt per pixel and the integration time is 19 msec.*

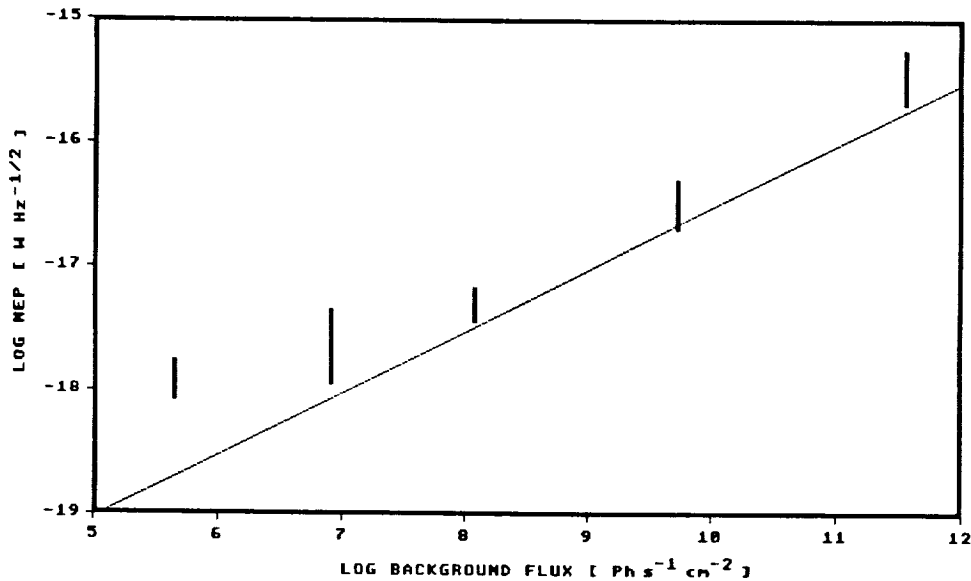


**Figure 6 Summary of NEP Measurements of the 10 x 50 Array**

*By using different sets of cold attenuation filters the background was varied over 6 orders of magnitude. The vertical bars indicate the range of NEP found by using various integration times (1 to 4000 msec) and bias voltages (up to 4.5V). Also different algorithms for data evaluation like statistical analysis and Fourier transformation have been applied. At background fluxes down to about  $10^7 \text{ Ph s}^{-1} \text{ cm}^{-2}$  the lower end of these bars where the operating parameters are optimized, coincide well with the BLIP-limit calculated with  $\eta = 0.5$ . At lower backgrounds the deviation from that limit indicates the influence of the readout noise.*



NEP and responsivity were almost independent of temperature below 4 Kelvin as shown in table 1. The dark current was measured at pixel #25 of rows 1,3,5 and 9 at a bias voltage of 4V. The results are shown in table 2. The linearity over integration time and infrared flux is shown in figures 7 and 8. A qualitative test of the crosstalk is shown in figure 9.

**Table 1 Temperature Dependence**

$Q_B$ [Ph s <sup>-1</sup> cm <sup>-2</sup> ]	$V_b$ [V]	$T_D$ [K]	$t_{int}$ [msec]	NEP [W Hz <sup>-1/2</sup> ]	R [AW <sup>-1</sup> ]
8.2 10 <sup>6</sup>	4.0	4.7	75	2.7 10 <sup>-18</sup>	570
	4.0	3.6	75	2.4 10 <sup>-18</sup>	900
	4.0	3.2	75	2.2 10 <sup>-18</sup>	920
	4.0	3.0	75	2.1 10 <sup>-18</sup>	900

**Table 2 Dark Current at 4V Bias**

Pixel	Dark Current [ Electrons / Second ]	
	T = 4.2 K	T = 3.1 K
1 , 25	63 700	16 300
3 , 25	64 400	16 800
5 , 25	63 200	15 900
9 , 25	61 000	14 800

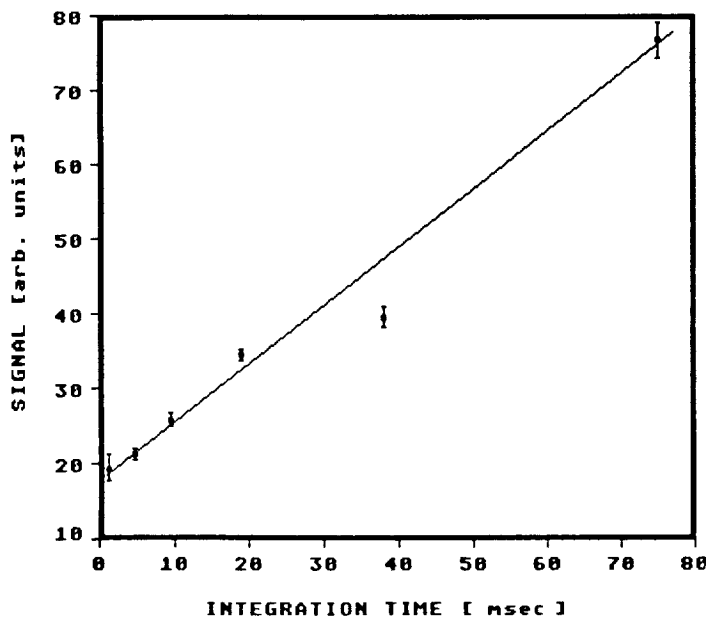


**Figure 7**

**Linearity over Integration Time**

*Except for the integration at 38msec the signal is linear in time within the measurement's accuracy.*

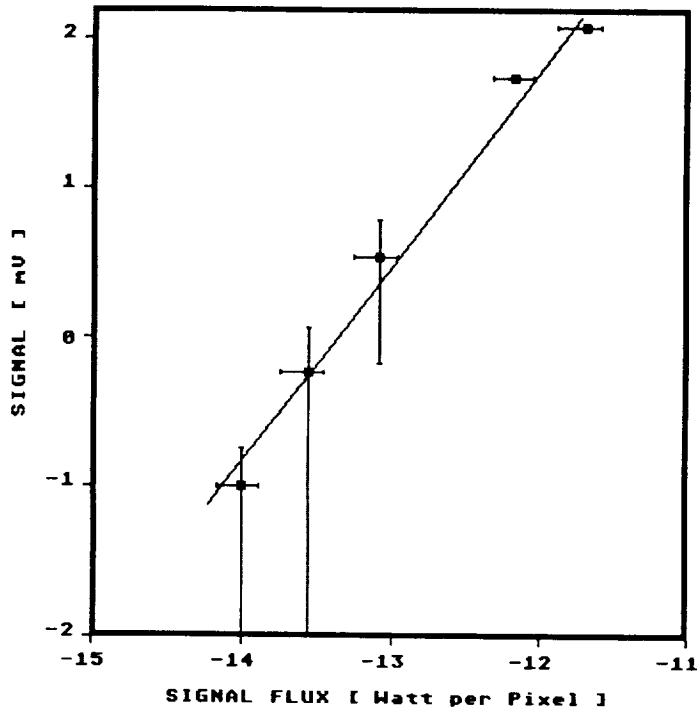


**Figure 8**  
**Linearity in Infrared Flux**

*At low fluxes the noise of the output voltage gives large error bars which disappear at the higher signals. The errors in flux are caused by the uncertainty of the attenuation filter's cold spectral transmission. Within these limits the detector is linear.*

#### Conclusion

Although the data presented here are not a complete investigation of the devices, the excellent suitability of these arrays for space astronomy is obvious. With a NEP of about  $10^{-18} \text{ WHz}^{-1/2}$  the  $10 \times 50$  array offers a factor  $\sim 10$  better sensitivity compared to bulk detectors at photon background fluxes below  $10^7 \text{ Phs}^{-1} \text{ cm}^{-2}$ . Its very high responsivity of  $\sim 1000 \text{ AW}^{-1}$  makes the use of a relatively noisy readout circuit possible. Besides these sensitivity advantages, the high energy radiation immunity of these detectors would be a great gain for a space astronomy. We very much regret that this technology could not be made available for the use in our ISOPHOT experiment.

#### Acknowledgement

The export license for the two detector arrays authorized testing for a 10 months loan period in our lab. We are very grateful to C. D. Lawson of Rockwell International in Anaheim for the big amount of work he put into obtaining that license. During set-up of our tests we got valuable help from the staff of the Rockwell Science Center, Anaheim. We appreciate very much the open discussions of our technical problems and the advices we got. We also thank the staff of the machine shop in our institute for the quick delivery of test equipment. Finally we want to thank C.R. McCreight for his support to include this presentation in his workshop.

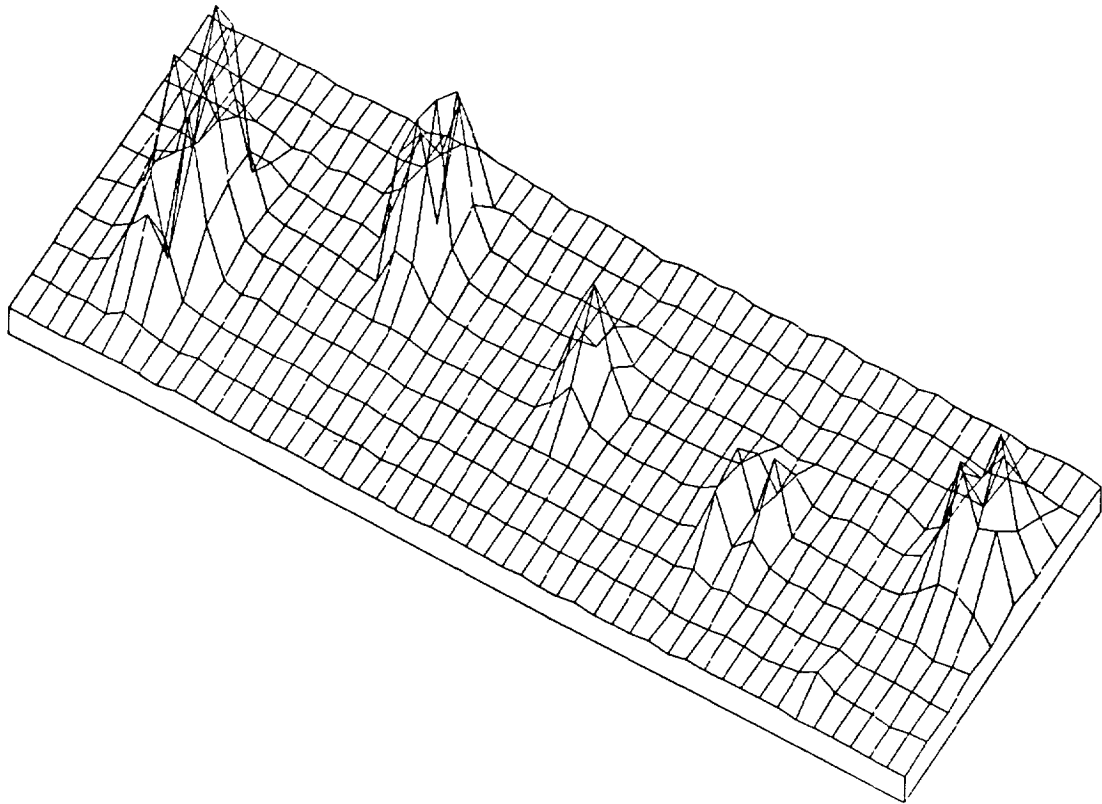


**Figure 9 Crosstalk Test**

*To test the crosstalk of the array a blackened mask was put within 1 mm close to its surface. Through holes ranging from 0.2 to 0.5 mm in diameter small areas of the array were illuminated. We did not attempt a quantitatively evaluate this but the steep slopes of the "light-mountains" indicate low crosstalk. For this plot an integration looking at the cold shutter was used for flat-fielding.*

#### References

1. Wolf, J., Lemke, D., Burgdorf, M., Grözinger, U., Hajduk, Ch.: "Status of the ISOPHOT Detector Development", this conference
2. Stetson, S.B., Reynolds, D.B., Stapelbroek, M.G., Stermer, R.L.: "Design and performance of blocked-impurity-band detector focal plane arrays", Proc. SPIE, 686, 48 (1986)



## Report Documentation Page

1. Report No. NASA TM-102209	2. Government Accession No.	3. Recipient's Catalog No.	
4. Title and Subtitle Proceedings of the Third Infrared Detector Technology Workshop		5. Report Date October 1989	6. Performing Organization Code
		8. Performing Organization Report No. A-89200	
7. Author(s) The authors and their affiliations are shown in the list of attendees		10. Work Unit No. 506-45-31	11. Contract or Grant No.
		9. Performing Organization Name and Address Ames Research Center Moffett Field, CA 94035	
12. Sponsoring Agency Name and Address National Aeronautics and Space Administration Washington, DC 20546-0001		13. Type of Report and Period Covered Technical Memorandum February 7-9, 1989	
		14. Sponsoring Agency Code	
15. Supplementary Notes Point of Contact: Craig R. McCreight, Ames Research Center, MS 244-10, Moffett Field, CA 94035 (415) 694-6549 or FTS 464-6549			
16. Abstract This volume consists of 37 papers which summarize results presented at the Third Infrared Detector Technology Workshop, held February 7 - 9, 1989, at Ames Research Center. The workshop focused on infrared (IR) detector, detector array, and cryogenic electronic technologies relevant to low-background space astronomy. Papers on discrete IR detectors, cryogenic readouts, extrinsic and intrinsic IR arrays, and recent results from ground-based observations with integrated arrays were given. Recent developments in the second-generation Hubble Space Telescope (HST) infrared spectrometer and in detectors and arrays for the European Space Agency's Infrared Space Observatory (ISO) are also included, as are status reports on the Space Infrared Telescope Facility (SIRTF) and the Stratospheric Observatory for Infrared Astronomy (SOFIA) projects.			
17. Key Words (Suggested by Author(s)) Infrared detectors Infrared detector arrays Cryogenic electronics Infrared astronomy		18. Distribution Statement Unclassified-Unlimited  Subject Category - 35	
19. Security Classif. (of this report) Unclassified	20. Security Classif. (of this page) Unclassified	21. No. of Pages 474	22. Price A20



